Title

Zwitterionic PEG-PC Hydrogels Modulate the Foreign Body Response in a Modulus-Dependent Manner

Journal

Biomacromolecules, 19(7)

ISSN

1525-7797

Authors

Jansen, Lauren E
Amer, Luke D
Chen, Esther Y-T
et al.

Publication Date

2018-07-09

DOI

10.1021/acs.biomac.8b00444

Peer reviewed

HHS Public Access

Author manuscript

Biomacromolecules. Author manuscript; available in PMC 2019 July 09.

Published in final edited form as:

Biomacromolecules. 2018 July 09; 19(7): 2880–2888. doi:10.1021/acs.biomac.8b00444.

Zwitterionic PEG-PC hydrogels modulate the foreign body response in a modulus-dependent manner

Lauren E. Jansen[1], **Luke D. Amer**[2], **Esther Y-T Chen**[3], **Thuy V. Nguyen**[1], **Leila S. Saleh**[2], **Todd Emrick**[4], **Wendy F. Liu**[3], **Stephanie J. Bryant**[2], and **Shelly R. Peyton**[1,*]

[1]University of Massachusetts, Amherst, Department of Chemical Engineering

[2]University of Colorado Boulder, Department of Chemical and Biological Engineering

[3]University of California, Irvine, Department of Biomedical Engineering

[4]University of Massachusetts, Amherst, Department of Polymer Science and Engineering

Abstract

Reducing the foreign body response (FBR) to implanted biomaterials will enhance their performance in tissue engineering. Poly(ethylene glycol) (PEG) hydrogels are increasingly popular for this application due to their low cost, ease of use, and the ability to tune their compliance via molecular weight and crosslinking densities. PEG hydrogels can elicit chronic inflammation *in vivo*, but recent evidence has suggested that extremely hydrophilic, zwitterionic materials and particles can evade the immune system. To combine the advantages of PEG-based hydrogels with the hydrophilicity of zwitterions, we synthesized hydrogels with co-monomers PEG and the zwitterion phosphorylcholine (PC). Recent evidence suggests that stiff hydrogels elicit increased immune cell adhesion to hydrogels, which we attempted to reduce by increasing hydrogel hydrophilicity. Surprisingly, hydrogels with the highest amount of zwitterionic co-monomer elicited the highest FBR we observed. Lowering the hydrogel modulus (165 kPa to 3 kPa), or PC content (20 wt% to 0 wt%), mitigated this effect. A high density of macrophages was found at the surface of implants associated with a high FBR, and mass spectrometry analysis of the proteins adsorbed to these gels implicated extracellular matrix, immune response, and cell adhesion protein categories as drivers of macrophage recruitment to these hydrogels. Overall, we show that modulus regulates macrophage adhesion to zwitterionic-PEG hydrogels, and demonstrate that chemical modifications to hydrogels should be studied in parallel with their physical properties to optimize implant design.

[*]**Corresponding Author:** speyton@ecs.umass.edu.

Author Contributions

All authors contributed to experimental design, data analysis, and wrote the manuscript. LEJ, EY-TC, TVN, LSS, and LDA performed all the experiments.

ASSOCIATED CONTENT

Supporting Information

Further characterization of protein adsorption onto hydrogels, fibrous capsule collagen density, and macrophage adhesion and response to cytokines is available in the supplemental information. In addition, all the raw LC-MS protein data from each biomaterials and the hierarchical clustering code is available.

Keywords

extracellular matrix; proteomics; macrophages; tissue engineering

1. Introduction

Poly(ethylene glycol) (PEG) hydrogels are used in tissue engineering because they are compatible with cells, and they are easy to chemically functionalize. These features make them attractive biomaterials to control cell growth, migration, and tissue regeneration via porosity[1–2], stiffness[3–4], and presentation of peptides and proteins[5–7]. Though PEG hydrogels have been used extensively *in vitro* to culture chondrocytes[8], mesenchymal stem cells[1], hepatocytes[9], and muscle cells[3], the capacity for these cells to regenerate functional tissues could be limited *in vivo* because PEG hydrogels elicit a foreign body response (FBR)[10]. The FBR to implanted materials starts with protein adsorption to the biomaterial surface, which facilitates macrophage adhesion[11]. Pro-inflammatory macrophages and foreign body giant cells (FBGCs) can then recruit other cells, such as fibroblasts[12], or take on a myofibroblast phenotype themselves[13–14], and deposit collagen around the implants[15]. This matrix remodeling ultimately leads to fibrosis and chronic inflammation. The mechanism of the FBR to PEG hydrogels is proposed to be driven by either its susceptibility to degradation by macrophages[10], or because certain inflammatory proteins can adhere to the hydrogel surface[16]. Since PEG degradation leads to surface fouling and protein adsorption[17], these properties are potentially coupled.

Recent work has shown that the size, shape, stiffness, and charge of implanted materials have a profound impact on the FBR[18–20]. For example, large, spherical hydrogels in a colloidal implant exhibit less fibrosis than small ones[20]. Also, increasing hydrogel stiffness increases the collagen capsule thickness around PEG hydrogel implants, likely because macrophages are better able to adhere and spread on stiffer hydrogels[19]. Stiffness-driven FBR is a concern, because the ability to regenerate different tissues, like muscle, can rely on stiffness[3]. The FBR could be reduced by chemically modifying these stiff PEG hydrogels. Researchers have shown that including cell-adhesive[16] and enzyme-degradable peptides[5–6] reduce the FBR to PEG hydrogels, because they stimulate interactions with immune cells that promote wound healing.

An approach that has been used for other hydrogels, but not PEG, is surface chemical modification to avoid activating the immune system. For example, a combinatorial approach screened 774 different alginate analogs to identify formulations that reduced the FBR to implanted alginate hydrogels[21]. Polymer microparticles co-injected with anti-inflammatory drugs inhibit inflammatory proteases and reactive oxygen species[22]. Hydrogels made with the zwitterion carboxybetaine significantly reduced the immune response and implant FBR[18]. This study suggests that zwitterionic materials could be an effective way to reduce the FBR to otherwise inflammatory materials. Phosphorylcholine (PC) zwitterions are of particular interest because of their *in vivo* use as medical device coatings, and they have been shown to reduce immune cell adhesion[23–25]. Recently, we synthesized hydrogels composed of both PEG and PC, which have an increased range of stiffnesses, and reduced

protein adsorption *in vitro* compared to PEG-only hydrogels[26]. These PEG-PC hydrogels can be used for cell culture scaffolds of varying stiffness and biochemical complexity[27–29]. We hypothesized that PEG-PC hydrogels would have a reduced inflammatory response because of minimal protein adsorption, making them potentially advantageous for long-term *in vivo* implants. To test that hypothesis, we synthesized a panel of PEG-PC hydrogels with varying stiffness and zwitterion content to investigate how these two properties independently contribute to the FBR. Using both *in vitro* and *in vivo* assays, we explored how the chemical and physical compositions of hydrogels influence protein adsorption and macrophage polarization, and ultimately how these properties modulate the FBR.

2. Materials and Methods

2.1 Hydrogel fabrication

PEG-PC hydrogels were polymerized as previously described[26]. In brief, PEG dimethacrylate and 2-methacryloyloxyethyl phosphorylcholine (PC) (Sigma-Aldrich, St. Louis, MO) were dissolved in PBS at the concentrations shown in Table 1. Pre-polymer solutions were degassed with nitrogen for 30 seconds and cured under UV light (365 nm, average intensity of 6.7 mW/cm^2, UV Panel HP, American DJ, Los Angeles, CA) with 0.8 wt% of Irgacure 2959 (BASF, Ludwigshafen, Germany). UV-light intensity was measured with a Digital UV Meter (Solartech Inc. Model 5.0 UVA + B, serial No. 17893). For *in vivo* implantation, hydrogels were formed under sterile conditions in a 5 mm diameter by 0.8 mm height cylindrical mold and swollen overnight in PBS (final surface area ranged between 60–120 mm^2). For *in vitro* studies, hydrogels were swollen in PBS overnight and punched into 6 mm diameter discs with an average height of 0.5 mm.

2.2 In vivo hydrogel implants

Hydrogel disks were implanted subcutaneously into the dorsal pockets of eight-week-old C57BL/6 male mice (Charles River Laboratories, Wilmington, MA) by making a subcutaneous incision along the centerline of the back shoulder blades. Hydrogels were left *in vivo* for 30 minutes for short-term protein adsorption studies, and for 28 days for quantification of fibrous capsule formation and macrophage recruitment. Each animal received four implants, each implant consisting of unique hydrogel chemistry. Both hydrogel chemistry and location of biological replicates were randomized on the backs of each mouse (N=4 for each variation of hydrogel implanted). Endotoxin levels were measured using the ToxinSensor Chromogenic LAL Endotoxin Assay Kit according to the manufacturer's instructions (Genscript, China).

2.3 Animal protocols

All animal protocols were in accordance with NIH guidelines for animal handling and approved by the University of California Irvine, the University of Massachusetts Amherst, and the University of Colorado at Boulder Institutional Animal Care and Use Committees.

2.4 Protein adsorption

Hydrogel implants were explanted after 30 minutes of incubation *in vivo* to determine initial protein adsorption to gel surfaces. Hydrogels were incubated for 30 minutes in 10% fetal

bovine serum (FBS) (Thermo Fisher Scientific, Waltham, MA) in PBS for *in vitro* protein adsorption. To remove and quantify the adsorbed proteins, hydrogels were soaked in 50 mM ammonium bicarbonate (Thermo) solution for 2 hours. Solutions were removed and either immediately processed, or flash frozen and stored at −80°C until processing. *In vitro* gels were additionally incubated with 1 wt% SDS (Hoefer, Holliston, MA) for 30 minutes, and solutions were immediately processed. Total protein concentration was measured using a bicinchoninic acid assay (BCA) assay according to manufacturer's instructions (Thermo). Protein was loaded at 10 μg/lane, run on a 4–29% tris-glycine polyacrylamide gel, stained using silver stain according to manufacturer's instructions (Thermo), and imaged using the IN Genius Syngene Bioimaging platform (Frederick, MD).

2.5 Mass Spectrometry

Proteins removed from the explanted hydrogels were reduced in 10 mM dithiothreitol (DTT) (Thermo) for 30 minutes at 37°C. Samples were alkylated with 20 mM iodoacetamide (Sigma-Aldrich) in the dark at room temperature for 30 minutes. The solution was quenched with 5 mM DTT prior to cleavage. Proteins were cleaved via trypsin (Thermo) and Lys-C endoproteinase (Promega, Madison, WI) at a ratio of 1:50 enzyme to protein overnight (12–16 hours) at 37°C. A reverse phase LC gradient was used to separate peptides prior to analysis. Mass spectrometry analysis was performed in an Orbitrap Fusion Tribrid (Thermo). Peptides were aligned against the UniProt *Mus musculus* proteome using the Thermo Proteome Discoverer 1.41.14. Parameters used trypsin as a protease, with 4 missed cleavages per peptide, a precursor mass tolerance of 10 ppm, and fragment tolerance of 0.6 Da. Proteins identified had a PSM>1, coverage >10%, unique peptides >1, and a protein score >0 (protein score is developed by Proteome Discoverer to indicate confidence for a protein hit). Of these hits, only full-length proteins identified on at least two of the three hydrogel replicates are reported for each sample condition. Hierarchical clustering analysis was performed using the MATLAB Bioinformatics toolbox R2015b (Mathworks, Natick, MA) on the proteins removed from explanted hydrogels and identified through mass spectrometry. Euclidean distance and average linkage were used to generate the dendrogram. Data were normalized by giving proteins present on the hydrogel a value of 1 and proteins absent a value of 0. The MATLAB code for hierarchical clustering is available at openwetware.org/wiki/Peyton:Internal.

2.6 Gene Ontology

The Database for Annotation, Visualization, and Integrated Discovery (DAVID) v6.7 (http://david.abcc.ncifcrf.gov/)[30–31] was used to assess the biological process and cellular component gene ontology terms associated with each of the identified proteins. All proteins identified across the substrates were submitted as background and the individual protein hits for each hydrogel were compared to find gene ontology groups. Notable ontology groups are highlighted, and the p-values are reported.

2.7 Histological analysis

Swartzlander et al. have previously described the tissue preparation, imaging, and image analysis used here[16]. Briefly, hydrogels were explanted alongside the dorsal skin, fixed in paraformaldehyde, and embedded in paraffin. Samples (10 μm thick) were stained with

Masson's Trichrome via standard protocols. Collagen density was measured using the protocol published by Zhang et al.[18]. Macrophages were stained with the rat anti-mouse Mac3 as the primary antibody (1:30, Abcam, Cambridge, MA) and the biotin anti-rat IgG (1:30, Abcam).

2.8 Primary macrophage adhesion

Monocytes were isolated from the bone marrow of 7 to 10 week-old C57BL/6 male mice (Jackson Laboratory, Bar Harbor, ME) as described previously[32]. Cells were separated using Lympholyte M (Accurate Chemical, Westbury, NY) and plated in macrophage differentiation medium (IMDM with 20% FBS, 2 mM L-glutamine (Thermo), 1% penicillin-streptomycin (Corning, Corning, NY), 1.5 ng/ml recombinant mouse macrophage colony stimulating factor (M-CSF, R&D Systems, Minneapolis, MN), and 100 ng/ml flt-3 ligand (R&D Systems) for 5 days. Macrophages were lifted from culture plates using a cell scraper and 0.05% trypsin-EDTA. A soybean trypsin inhibitor (Thermo) was used in place of serum. Cells were seeded at 30,000 cells/cm^2 in serum-free medium on hydrogels swollen in PBS or in 10% FBS in PBS, Human Plasma Fibronectin (Millipore, Billerica, MA), Collagen I from rat tail (Thermo), or active mouse Fibrinogen protein (ab92791, Abcam) for 30 minutes prior to seeding. After 24 hours, hydrogels were rinsed, fixed in 4% formaldehyde, and adhered macrophages were stained with DAPI at 1:10000 (Thermo). Adhered macrophages were imaged on a Zeiss Axio Observer Z1 microscope (Carl Zeiss, Oberkochen, Germany) using an AxioCam MRm camera and an EC Plan-Neofluar 20X 0.4 NA air objective and manually quantified using ImageJ (NIH, Bethesda, MD).

2.9 Assessment of cytokine secretion

Bone marrow-derived macrophages used in the cytokine secretion assay were harvested from the femurs and tibias of 6–10 week-old C57BL/6 mice (Jackson Laboratory) as previously described[33]. Briefly, cells were treated with ACK lysis buffer (Thermo), centrifuged, and resuspended in culture medium containing 10% heat-inactivated FBS and recombinant M-CSF for macrophage differentiation. BMDM were dissociated using cell dissociation buffer (Invitrogen) and scrapers on day 6–8 and seeded on the gels in culture media. Cells were seeded in a 24-well plate at 400,000 cells/well. 6 hours after cell seeding, the culture media was replaced with one of the four conditioning media: 1) no stimulation, 2) 1 ng/mL of LPS/IFN-ϒ (Sigma and BioLegend, San Diego, CA) each, 3) 20 ng/mL IL-4/IL-13 (BioLegend) each, and 4) 0.5 ng/mL LPS and 20 ng/mL IL-4/IL-13 each. After 12 hours of incubation, the supernatants were collected and analyzed for TNF-α and IL-10 secretion by enzyme-linked immunosorbent assay (ELISA) following the manufacturer's instructions (BioLegend).

2.10 Statistical Analysis

Statistical analysis was performed using GraphPad's Prism v7.0a (La Joya, CA). Statistical significance was evaluated using either a two-tailed t-test or a one-way analysis of variance where noted, followed by a Tukey's post-test for pairwise comparisons. All biological replicates (N) and technical replicates (n) for each experiment are indicated in the figure legends. A minimum of 2 biological and 3 technical replicates were used for each experiment. Spearman correlations were calculated from means and standard deviations

paired by the condition. P-values <0.05 are considered significant, where p<0.05 is denoted with *, ≤0.01 with **, and ≤0.001 with ***.

3. Results

3.1 The zwitterion phosphorylcholine increases the FBR to PEG hydrogels

We explored the interplay between hydrogel modulus and zwitterionic content, two parameters that separately regulate the immune response to hydrogel implants. Using our PEG-PC hydrogel[26], we created a panel of conditions that independently modulated either hydrogel modulus or zwitterion content (Table 1). Hydrogel modulus was either increased from ~3 to 165 kPa by adding PEG while PC content was kept at 20 wt%, or the average moduli was held between 160–175 kPa by adding PEG to compensate for the modulus loss while PC was decreased from 20 to 0 wt% (Figure 1a–b). The soft, high PC hydrogels swelled the most, and hydrogel swelling decreased with increasing stiffness and removal of the PC zwitterion (Figure 1c). These hydrogels, which had low endotoxin levels (<0.08 EU/mL), were implanted into C57BL/6 mice for 28 days. We first observed that with a fixed zwitterion content, increasing the stiffness by adding more PEG increased the thickness of the fibrous capsule, a result consistent with previous findings (conditions A-C in Figure 1d–e)[19]. Surprisingly, reducing the amount of zwitterion, while holding the hydrogel modulus at the maximum tested here, decreased the fibrous capsule thickness (conditions C-F in Figure 1d–e). Though both hydrogel stiffness and PC content contributed to the final thickness of the collagen capsule, the collagen density throughout the capsule was not significantly different among any of the hydrogels (Suppl. Figure 1).

3.2 Proteins associated with the extracellular matrix are enriched on the high FBR hydrogel

One of the first steps in the FBR is the formation of a provisional protein matrix[15]. We previously showed that the addition of PC to PEG hydrogels decreases protein adsorption to hydrogels *in vitro*[26], and decreasing non-specific protein adsorption with zwitterions has been proposed by others to reduce the FBR[18]. We quantified the total protein adsorbed to the surface of our hydrogels (Table 1) during *in vitro* exposure to serum to see if this explained our observation of the enhanced FBR on the stiffest, most zwitterionic hydrogels. In both *in vivo* and *in vitro* experiments, we observed that the softest hydrogel condition, which exhibited the lowest FBR, had the greatest protein accumulation (Figure 2a–b). Thus, total adsorbed protein could not explain the FBR to our array of hydrogels.

Both of these methods demonstrated that adding zwitterion did not decrease the total amount of protein adsorbed to hydrogels, which contradicted our original hypothesis. We then used a series of more rigorous rinse methods to determine the degree of loosely bound protein. When a phosphate buffered saline (PBS) wash was added before protein removal with ammonium bicarbonate (Suppl. Figure 2a), we found that ~75% of the total protein was removed. This indicates that most of the protein was adsorbed passively on the hydrogel surfaces and not tightly bound. We also added a final wash with sodium dodecyl sulphate (SDS), and found that a minimal amount of protein could be detected on the hydrogels post-washing with ammonium bicarbonate (Figure 2c). The presence of PC appeared to reduce

the strength of protein adsorption to the hydrogels. We speculated that smaller proteins might be diffusing into the softest, most porous hydrogels (condition A in particular, see Figure 1c and 2d). In fact, the mesh size of our hydrogels correlated with the total protein adsorption during gentle rinsing (Suppl. Figure 2b, Spearman ρ=0.94, p=0.016). Overall, these results indicate that the increased protein adsorption (Figures 2a–b) may be driven by protein diffusion into the network, and that zwitterions impact protein binding strength.

Since total protein adsorption did not correlate with the observed FBR, we next examined whether the identity of the proteins adhered to the hydrogels could predict the FBR. Using a silver stain, we were unable to distinguish any major differences in the protein molecular weight signature adsorbed to the implanted *in vivo* hydrogels (Suppl. Figure 3a). From the more sensitive liquid chromatography-mass spectrometry (LC-MS) technique, we annotated over 350 of the proteins that adsorbed to each hydrogel surface 30 minutes after *in vivo* implantation (Figure 3a, Suppl. Table 1). This time point has been used in previous studies of protein adsorption to hydrogels because it is before most cells adhere to the implants *in vivo*[16]. The majority of the top 20 protein hits were conserved across all the hydrogels, in agreement with our silver stain results (Suppl. Table 2, Suppl. Figure 3b). Unsupervised hierarchical clustering of protein hits identified using LC-MS separated hydrogels by either high stiffness or high zwitterion content (Figure 3b, separation indicated by Euclidean distance). We did observe a correlation between mesh size and *in vitro* protein adsorption, and many of the proteins we quantified have been reported to diffuse rapidly out of PEG hydrogels with a similar mesh size[34–35]. LC-MS was also unable to identify any appreciable trends in protein molecular weights adhered to each hydrogel (Suppl. Figure 3c). However, our LC-MS results showed that a higher percentage of proteins with extreme isoelectric points (above 9 and below 5) adsorbed to the stiffer hydrogels containing PC, compared to hydrogels with low or no PC included (Suppl. Figure 3d–e).

It is well known that hydrogel surface chemistries can influence protein adsorption[36–37]. Given that clustering of proteins distinguished the higher zwitterionic content from the stiffest hydrogel conditions, we hypothesized that a subset of proteins could be identified that were recognized by immune cells and drove the observed FBR. A DAVID analysis identified categories of proteins associated with biological processes and cell components that adsorbed onto the hydrogels with the maximum (C) and minimum (A and F) collagen capsule thickness. We focused our search on categories associated with cell and immune response, extracellular matrix (ECM), and ECM remodeling, because we speculated these categories could explain the formation of the fibrous capsule. In fact, a higher percentage of proteins from these categories were found on the high FBR hydrogel compared to the others, as confirmed by more significant p-values (Figure 3c).

3.3 Stiffer hydrogels with higher PC promote an inflammatory phenotype in macrophages

Macrophages are one of the most prominent cell types that accumulate rapidly to the surface of implanted materials and devices, and they play a major role in initiating chronic inflammation[38]. We hypothesized that macrophage adhesion to the proteins we detected via LC-MS may drive the observed FBR response to the stiffer, more zwitterionic hydrogels. Therefore, we examined macrophages present near the implants *in vivo* and performed a

macrophage adhesion experiment *in vitro*. The extent of macrophage infiltration around implanted hydrogels *in vivo* was highest around the high FBR hydrogel (condition C, Figure 4a). Similarly, macrophage adhesion to these hydrogels *in vitro* was highest on this hydrogel condition (Figure 4b). Interestingly, this *in vitro* adhesion was only observed in the presence of serum, suggesting that protein adsorption to the surface of the gels is required for macrophage adhesion.

During the FBR, adhered macrophages recruit fibroblasts to the wound site to begin ECM turnover by releasing an array of cytokines[15]. Thus, we examined the medium for inflammatory cytokines secreted by macrophages attached to either the high FBR or the two lowest FBR hydrogels *in vitro* (conditions C vs. A and F, Figures 4c–d). Secretion of TNF-α is associated with pro-inflammatory macrophages, and IL-10 with anti-inflammatory macrophages[39–40]. These cytokines do not directly correlate to distinct states of macrophage activation, but can predict *in vivo* response. Macrophages secreted high quantities of IL-10, regardless of hydrogel condition (Figure 4c), but TNF-α secretion was highest on the hydrogel condition that produced the highest FBR (Figure 4d). Interestingly, cytokine secretion was independent of the polarizing stimuli added to the medium including LPS, IFN-γ, IL4, and IL13, which were confirmed to influence the amount and type of cytokine secreted when cells are cultured on tissue culture plastic (Figure 4c–d, Suppl. Figure 4a–b).

4. Discussion

Although PEG-based materials have been used widely in tissue engineering applications[41–42], recent studies have shown they elicit an inflammatory response[10]. This response can be reduced using zwitterions[18], one example being zwitterion-coated nanocarriers[43]. Here, we investigated whether inclusion of PC groups could reduce the FBR when incorporated into PEG hydrogels.

We developed a panel of hydrogels with varying amounts of PEG and PC to independently modulate stiffness and zwitterionic content (Figure 1a–c). Reducing the amount of PC in hydrogels while using PEG to keep the bulk hydrogel modulus constant decreased the fibrous capsule thickness, whereas increasing the amount of PEG crosslinker in hydrogels with a constant amount of PC increased the capsule thickness (Figure 1d–e). Stiffness-driven inflammation has been previously reported in PEG hydrogels, where increased crosslinking increased macrophage spreading on the surface[19], but not other systems like gelatin-derived hydrogels[44]. Surprisingly, the higher modulus hydrogels lacking zwitterions had a significantly lower FBR than the PEG-PC hydrogels with the same modulus. Others have reported that zwitterionic hydrogels reduce the FBR[18], but this previous work utilized much stiffer hydrogels than those explored here and did not study the impact of zwitterions when other physical/mechanical properties of hydrogels were varied. This is an important feature as stiffness is now well appreciated to drive cell behavior[45]. In light of our results, we propose that the stiffness of the material changes the immune response to the zwitterion PC by modulating protein adsorption and macrophage adhesion associated with FBR, and this should be tested for other ranges of stiffness and PC content. One potentially confounding aspect of the material used in this study was the need to balance stiffness and the amount of zwitterion to parse out the chemical and physical contributions. This led to different total

solid contents for the hydrogels studied. Of note, there was a correlation between total hydrogel solid content and capsule thickness (A 21%, B 24%, C 26%, D 23%, E 20%, F 18.4%, Spearman ρ=0.94, p=0.049), which may indicate that simply more implanted material led to the inflammatory macrophage response.

The thick layer of macrophages surrounding the high FBR hydrogel (Figure 4a) correlated with the collagen capsule thickness around the implant (Figure 1d). We further explored these results *in vitro* and observed that adhesion of macrophages was highest on our high FBR hydrogel (Figure 4b). The adhered macrophages also expressed significantly more TNF-α on this hydrogel compared to the two lowest FBR conditions (Figure 4c), suggesting that the adhered macrophages were more pro-inflammatory. These data demonstrate that hydrogel C promoted the most pro-inflammatory phenotype in macrophages, which may have caused them to orchestrate the highest FBR. Though not investigated in this study, many have shown that these early pro-inflammatory signals eventually lead to macrophage fusion, creating FBGC's, which would inhibit the function of the implant[15].

Hydrogel surface properties can influence macrophage phenotypes. For example, adding an RGD integrin-binding motif to PEG promotes macrophage adhesion and promotes a wound healing phenotype, effectively decreasing the collagen capsule around hydrogel implants[16]. Interestingly, stimulating macrophages with cytokines used to direct cell phenotype did not influence the cell expression of TNF-α when seeded onto our hydrogels, but did impact cell phenotypes on tissue culture plastic (Figure 4c–d, Suppl. Figure 4a–b). This result indicated that the surface properties of the hydrogels were more important contributors to directing macrophage phenotype than the cytokine cocktails typically used in the field. Additionally, because these hydrogels are not fully zwitterionic, we hypothesized that the surface chemistry of the material influenced protein absorption, because cell adhesion increased in the presence of serum (Figure 4b). Increased cell adhesion did not correlate with an increase in the total protein adsorbed on the hydrogel surface (Figure 4b and Figure 2), but instead was likely dictated by the specific subset of proteins adsorbed that we detected via LC-MS (Figure 3). Recent work has identified specific proteins from serum, like clusterin, that make nanocarriers stealthy *in vivo*[46], and others have shown that coating materials with specific proteins can inhibit the inflammatory response of macrophages[33, 47]. Some have also postulated that developing biocompatible materials should focus on decreasing the protein unfolding upon adsorption, not just minimizing the amount of protein with zwitterions[48]. Thus, protein type and how it is displayed might be more influential to the FBR than total protein amount. In support of this, we found that proteins with extreme isoelectric points adsorbed more to hydrogels with lower to no PC content, highlighting that chemical properties do impact the types of proteins that adsorb.

LC-MS performed on proteins stripped off implanted hydrogels identified over 350 proteins adsorbed to these hydrogels *in vivo*. Many of the protein hits were shared across all the hydrogels screened (Suppl. Figure 3a,b, Suppl. Table 2). The most abundant protein hit was albumin (Suppl. Table 1), known as the major protein that adsorbs to surfaces of implants and/or injected nanoparticles[16, 46, 49]. Hierarchical clustering of all the proteins separated the higher stiffness and higher PC content hydrogels. We speculate that this separation was driven by the repulsion of highly charged proteins on hydrogels with the higher PC content

(Suppl. Figure 3d). However, the differences between the types of proteins adhering to the hydrogels was greater than the proteins separating high and low PC hydrogels, indicated by the Euclidean distance. This highlighted that both the stiffness and the charges displayed on the hydrogel surface influenced the provisional proteins adsorbed. Unsurprisingly, other hits, like Vitamin D binding protein[50], Apolipoprotein A-I or A-IV[51], and hemopexin[52], are known to be associated with inflammation, which was likely initiated during the implant procedure.

Gene ontology on the protein hits revealed that categories associated with ECM, immune response, and cell adhesion were most associated with the high FBR conditions (Figure 3c). This suggests that the provisional matrix that assembled on these materials may facilitate the initial adhesion of macrophages. We independently screened three different ECM proteins identified in the protein hits, and found that they assisted with macrophage adhesion to our PEG-only hydrogel (Suppl. Figure 4c). Blood plasma does not follow the same fouling principles on PEG as single or binary protein solutions[53], potentially explaining why these single proteins did not produce the same adhesion result as the complex serum. In addition, the manner in which a protein is displayed on a surface can also influence how macrophages respond. For example, fibrinogen can stimulate macrophage inflammation in soluble form, but inhibit inflammation when displayed as a fibrin matrix[39]. Furthermore, PEG-hydrogels mixed with pericardium matrix promote more of the pro-inflammatory cytokine IL-10 than PEG mixed with any individual protein[54]. Our data shows that many of our top protein hits are consistent across the hydrogels (Suppl. Table 2), so the difference we see in macrophage response might be how stiffness and charged altered the way individual proteins were displayed rather than protein identity. Since the mechanism of protein fouling is different on hydrophilic versus hydrophobic surfaces[55–56], and we studied a range of hydrophilic hydrogels here, we speculate that the mechanism of fouling may have influenced macrophage activation via changes in protein display.

5. Conclusion

The FBR to PEG-PC hydrogels changes with respect to both the stiffness and zwitterionic content. Our high FBR hydrogel promoted higher secretion of TNF-alpha by macrophages *in vitro*, which agreed with the trend we observed in the *in vivo* collagen capsule thickness. We speculate that controlling which proteins adsorb to the material surface within the first 30 minutes of implantation is critical in modulating the FBR to PEG-based hydrogels. While many parameters can confound our understanding of the FBR to implanted biomaterials, this work demonstrates that both stiffness and zwitterion content can independently modulate the FBR. Overall, we identified that the physical properties of implanted materials should be studied in conjunction with chemical surface modifications to fully understand the subsequent immune response.

Supplementary Material

Refer to Web version on PubMed Central for supplementary material.

ACKNOWLEDGMENT

We would like to acknowledge Elizabeth Brooks and Carey Dougan for their assistance with the UV-light intensity measurements. This work was funded by an NIH New Innovator Award 1DP2CA186573–01 awarded to SRP and 1DP2DE023319–01 to WFL, and the NIH award #1R21AR064436 awarded to SB. SRP is a Pew Biomedical Scholar supported by the Pew Charitable Trusts. TVN and SRP were supported by a Barry and Afsaneh Siadat Career Development Award. LSS and LDA were supported by a graduate assistantship in areas of need from the Department of Education. Research reported in this publication was supported by the NIH Award #S10OD010645. The content is solely the responsibility of the authors and does not necessarily represent the official views of the National Institutes of Health.

REFERENCES

1. Peyton SR; Kalcioglu ZI; Cohen JC; Runkle AP; Van Vliet KJ; Lauffenburger DA; Griffith LG, Marrow-derived stem cell motility in 3D synthetic scaffold is governed by geometry along with adhesivity and stiffness. Biotechnol Bioeng 2011, 108 (5), 1181–93. [PubMed: 21449030]
2. Hollister SJ, Porous scaffold design for tissue engineering Nature Materials 2005, 4.
3. Gilbert PM; Havenstrite KL; Magnusson KE; Sacco A; Leonardi NA; Kraft P; Nguyen NK; Thrun S; Lutolf MP; Blau HM, Substrate elasticity regulates skeletal muscle stem cell self-renewal in culture. Science 2010, 329 (5995), 1078–81. [PubMed: 20647425]
4. Rape AD; Zibinsky M; Murthy N; Kumar S, A synthetic hydrogel for the high-throughput study of cell-ECM interactions. Nature Communications 2015, 6, 8129.
5. Amer LD; Bryant SJ, The In Vitro and In Vivo Response to MMP-Sensitive Poly(Ethylene Glycol) Hydrogels. Ann Biomed Eng 2016, 44 (6), 1959–69. [PubMed: 27080375]
6. Griffin DR; Weaver WM; Scumpia PO; Di Carlo D; Segura T, Accelerated wound healing by injectable microporous gel scaffolds assembled from annealed building blocks. Nat Mater 2015, 14 (7), 737–44. [PubMed: 26030305]
7. Rice JJ; Martino MM; De Laporte L; Tortelli F; Briquez PS; Hubbell JA, Engineering the regenerative microenvironment with biomaterials. Adv Healthc Mater 2013, 2 (1), 57–71. [PubMed: 23184739]
8. Schneider Margaret C., B. CA, Bryant Stephanie J., Characterization of the chondrocyte secretome in photoclickable poly(ethylene glycol) hydrogels. Biotechnol Bioeng 2017, 9999.
9. Underhill GH; Chen AA; Albrecht DR; Bhatia SN, Assessment of hepatocellular function within PEG hydrogels. Biomaterials 2007, 28 (2), 256–70. [PubMed: 16979755]
10. Lynn Aaron D., B. AK, Kyriakides Themis R., and Bryant Stephanie J., Temporal progression of the host response to implanted poly(ethylene glycol)-based hydrogels. J Biomed Mater Res A. 2011, 96 (4), 621–631. [PubMed: 21268236]
11. Klopfleisch R; Jung F, The pathology of the foreign body reaction against biomaterials. Journal of Biomedical Materials Research Part A 2016, 105 (3), 927–940. [PubMed: 27813288]
12. de la Oliva N; Navarro X; Del Valle J, Time course study of long-term biocompatibility and foreign body reaction to intraneural polyimide-based implants. J Biomed Mater Res A 2017, 106 (4), 746–757 [PubMed: 29052368]
13. Mooney J; Rolfe B; Osborne G; Sester D; van Rooijen N; Campbell G; Hume D; Campbell J, Cellular Plasticity of Inflammatory Myeloid Cells in the Peritoneal Foreign Body Response. Am J Pathol 2012, 176 (1), 369–80.
14. Mooney J; Summers K; Gongora M; Grimmond S; Campbell J; Hume D; Rolfe B, Transcriptional switching in macrophages associated with the peritoneal foreign body response. Immunol Cell Biol 2014, 92 (6), 518–26. [PubMed: 24638066]
15. Anderson JM; Rodriguez A; Chang DT, Foreign body reaction to biomaterials. Semin Immunol 2008, 20 (2), 86–100. [PubMed: 18162407]
16. Swartzlander MD; Barnes CA; Blakney AK; Kaar JL; Kyriakides TR; Bryant SJ, Linking the foreign body response and protein adsorption to PEG-based hydrogels using proteomics. Biomaterials 2015, 41, 26–36. [PubMed: 25522962]

17. Luk Yan-Yeung, K. M, and Mrksich Milan, Self-Assembled Monolayers of Alkanethiolates Presenting Mannitol Groups Are Inert to Protein Adsorption and Cell Attachment. Langmuir 2000, 16, 9604–9608.

18. Zhang L; Cao Z; Bai T; Carr L; Ella-Menye JR; Irvin C; Ratner BD; Jiang S, Zwitterionic hydrogels implanted in mice resist the foreign-body reaction. Nat Biotechnol 2013, 31 (6), 553–6. [PubMed: 23666011]

19. Blakney AK; Swartzlander MD; Bryant SJ, The effects of substrate stiffness on the in vitro activation of macrophages and in vivo host response to poly(ethylene glycol)-based hydrogels. J Biomed Mater Res A 2012, 100 (6), 1375–86. [PubMed: 22407522]

20. Veiseh O; Doloff JC; Ma M; Vegas AJ; Tam HH; Bader AR; Li J; Langan E; Wyckoff J; Loo WS; Jhunjhunwala S; Chiu A; Siebert S; Tang K; Hollister-Lock J; Aresta-Dasilva S; Bochenek M; Mendoza-Elias J; Wang Y; Qi M; Lavin DM; Chen M; Dholakia N; Thakrar R; Lacik I; Weir GC; Oberholzer J; Greiner DL; Langer R; Anderson DG, Size- and shape-dependent foreign body immune response to materials implanted in rodents and non-human primates. Nat Mater 2015, 14 (6), 643–51. [PubMed: 25985456]

21. Vegas AJ; Veiseh O; Doloff JC; Ma M; Tam HH; Bratlie K; Li J; Bader AR; Langan E; Olejnik K; Fenton P; Kang JW; Hollister-Locke J; Bochenek MA; Chiu A; Siebert S; Tang K; Jhunjhunwala S; Aresta-Dasilva S; Dholakia N; Thakrar R; Vietti T; Chen M; Cohen J; Siniakowicz K; Qi M; McGarrigle J; Lyle S; Harlan DM; Greiner DL; Oberholzer J; Weir GC; Langer R; Anderson DG, Combinatorial hydrogel library enables identification of materials that mitigate the foreign body response in primates. Nat Biotechnol 2016, 34 (3), 345–52. [PubMed: 26807527]

22. Dang TT; Thai AV; Cohen J; Slosberg JE; Siniakowicz K; Doloff JC; Ma M; Hollister-Lock J; Tang KM; Gu Z; Cheng H; Weir GC; Langer R; Anderson DG, Enhanced function of immuno-isolated islets in diabetes therapy by co-encapsulation with an anti-inflammatory drug. Biomaterials 2013, 34 (23), 5792–801. [PubMed: 23660251]

23. Ishihara K, Highly lubricated polymer interfaces for advanced artificial hip joints through biomimetic design. Polymer Journal 2015, 47, 585–597.

24. Iwasaki Y; Ishihara K, Phosphorylcholine-containing polymers for biomedical applications. Anal Bioanal Chem 2005, 381 (3), 534–46. [PubMed: 15723256]

25. Goreish HH; Lewis AL; Rose S; Lloyd AW, The effect of phosphorylcholine-coated materials on the inflammatory response and fibrous capsule formation:In vitro and in vivo observations. Journal of Biomedical Materials Research Part A 2004, 68 (1), 1–9. [PubMed: 14661243]

26. Herrick WG; Nguyen TV; Sleiman M; McRae S; Emrick TS; Peyton SR, PEG-phosphorylcholine hydrogels as tunable and versatile platforms for mechanobiology. Biomacromolecules 2013, 14 (7), 2294–304. [PubMed: 23738528]

27. Herrick WG; Rattan S; Nguyen TV; Grunwald MS; Barney CW; Crosby AJ; Peyton SR, Smooth Muscle Stiffness Sensitivity is Driven by Soluble and Insoluble ECM Chemistry. Cell Mol Bioeng 2015, 8 (3), 333–348. [PubMed: 26495043]

28. Nguyen TV; Sleiman M; Moriarty T; Herrick WG; Peyton SR, Sorafenib resistance and JNK signaling in carcinoma during extracellular matrix stiffening. Biomaterials 2014, 35 (22), 5749–59. [PubMed: 24726537]

29. McRae Page S; Parelkar S; Gerasimenko A; Shin DY; Peyton SR; Emrick T, Promoting cell adhesion on slippery phosphorylcholine hydrogel surfaces. J. Mater. Chem. B 2014, 2 (6), 620–624.

30. Huang da W; Sherman BT; Lempicki RA, Bioinformatics enrichment tools: paths toward the comprehensive functional analysis of large gene lists. Nucleic Acids Res 2009, 37 (1), 1–13. [PubMed: 19033363]

31. Huang da W; Sherman BT; Lempicki RA, Systematic and integrative analysis of large gene lists using DAVID bioinformatics resources. Nat Protoc 2009, 4 (1), 44–57. [PubMed: 19131956]

32. Jay SM; Skokos E; Laiwalla F; Krady MM; Kyriakides TR, Foreign body giant cell formation is preceded by lamellipodia formation and can be attenuated by inhibition of Rac1 activation. Am J Pathol 2007, 171 (2), 632–40. [PubMed: 17556592]

33. Chen EY; Chu S-H; Gov L; Kim YK; Lodoen MB; Tenner AJ; Liu WF, CD200 modulates macrophage cytokine secretion and phagocytosis in response to poly(lactic-co-glycolic acid)

microparticles and films. Journal of Materials Chemistry B 2017, 5 (8), 1574–1584. [PubMed: 28736613]

34. Rehmann MS; Skeens KM; Kharkar PM; Ford EM; Maverakis E; Lee KH; Kloxin AM, Tuning and Predicting Mesh Size and Protein Release from Step Growth Hydrogels. Biomacromolecules 2017, 18 (10), 3131–3142. [PubMed: 28850788]
35. Zustiak SP; Leach JB, Characterization of protein release from hydrolytically degradable poly(ethylene glycol) hydrogels. Biotechnol Bioeng 2011, 108 (1), 197–206. [PubMed: 20803477]
36. Jones JA; Chang DT; Meyerson H; Colton E; Kwon IK; Matsuda T; Anderson JM, Proteomic analysis and quantification of cytokines and chemokines from biomaterial surface-adherent macrophages and foreign body giant cells. Journal of Biomedical Materials Research Part A 2015, 83 (3), 585–596.
37. Damanik FFR, Rothuizen TC, van Blitterswijk C, Rotmans JI & Moroni L, Towards an in vitro model mimicking the foreign body response: tailoring the surface properties of biomaterials to modulate extracellular matrix. Sci. Rep 4, 6325 (2014). Scientific Reports 2014, 4 (6325).
38. Dondossola E; Holzapfel B; Alexander S; Filippini S; Hutmacher D; Friedl P, Examination of the foreign body response to biomaterials by nonlinear intravital microscopy. Nature Biomedical Engineering 2016, 1 (0007).
39. Hsieh JY; Smith TD; Meli VS; Tran TN; Botvinick EL; Liu WF, Differential regulation of macrophage inflammatory activation by fibrin and fibrinogen. Acta Biomater 2017, 47, 14–24. [PubMed: 27662809]
40. Sridharan R; Cameron AR; Kelly DJ; Kearney CJ; O'Brien FJ, Biomaterial based modulation of macrophage polarization: a review and suggested design principles. Materials Today 2015, 18 (6), 313–325.
41. Magin CM; Alge DL; Anseth KS, Bio-inspired 3D microenvironments: a new dimension in tissue engineering. Biomed Mater 2016, 11 (2), 022001. [PubMed: 26942469]
42. Briquez PS; Clegg LE; Martino MM; Gabhann FM; Hubbell JA, Design principles for therapeutic angiogenic materials. Nature Reviews Materials 2016, 1 (1), 15006.
43. Yesilyurt V; Veiseh O; Doloff JC; Li J; Bose S; Xie X; Bader AR; Chen M; Webber MJ; Vegas AJ; Langer R; Anderson DG, A Facile and Versatile Method to Endow Biomaterial Devices with Zwitterionic Surface Coatings. Adv Healthc Mater 2017, 6 (4).
44. Yu T; Wang WY; Nassiri S; Kwan T; Dang C; Liu W; Spiller K, Temporal and spatial distribution of macrophage phenotype markers in the foreign body response to glutaraldehyde-crosslinked gelatin hydrogels J Biomater Sci Polym Ed 2016, 27 (8), 721–742. [PubMed: 26902292]
45. Marklein RA; Burdick JA, Controlling stem cell fate with material design. Adv Mater 2010, 22 (2), 175–89. [PubMed: 20217683]
46. Schottler S; Becker G; Winzen S; Steinbach T; Mohr K; Landfester K; Mailander V; Wurm FR, Protein adsorption is required for stealth effect of poly(ethylene glycol)- and poly(phosphoester)-coated nanocarriers. Nat Nanotechnol 2016 11, 372–377. [PubMed: 26878141]
47. Kim YK; Que R; Wang SW; Liu WF, Modification of biomaterials with a self-protein inhibits the macrophage response. Adv Healthc Mater 2014, 3 (7), 989–94. [PubMed: 24573988]
48. Blaszykowski C; Sheikh S; Thompson M, Biocompatibility and antifouling: is there really a link?. Trends in Biotechnology 2013, 32 (2), 61–62. [PubMed: 24321373]
49. Tenzer S; Docter D; Kuharev J; Musyanovych A; Fetz V; Hecht R; Schlenk F; Fischer D; Kiouptsi K; Reinhardt C; Landfester K; Schild H; Maskos M; Knauer SK; Stauber RH, Rapid formation of plasma protein corona critically affects nanoparticle pathophysiology. Nat Nanotechnol 2013, 8 (10), 772–81. [PubMed: 24056901]
50. Prietl B; Treiber G; Pieber TR; Amrein K, Vitamin D and immune function. Nutrients 2013, 5 (7), 2502–21. [PubMed: 23857223]
51. Yu BL; Wang SH; Peng DQ; Zhao SP, HDL and immunomodulation: an emerging role of HDL against atherosclerosis. Immunol Cell Biol 2010, 88 (3), 285–90. [PubMed: 20065996]
52. Vinchi F; Silva M. C. d.; Ingoglia G; Petrillo S; Brinkman N; Zuercher A; Cerwenka A; Tolosano E; Muckenthaler MU, Hemopexin therapy reverts heme-induced proinflammatory phenotypic switching of macrophages in a mouse model of sickle cell disease. Blood 2016, 28, 473–486.

53. Riedel T; Riedelova-Reicheltova Z; Majek P; Rodriguez-Emmenegger C; Houska M; Dyr JE; Brynda E, Complete identification of proteins responsible for human blood plasma fouling on poly(ethylene glycol)-based surfaces. Langmuir 2013, 29 (10), 3388–97. [PubMed: 23391268]

54. Bracaglia LG; Messina M; Winston S; Kuo CY; Lerman M; Fisher JP, 3D Printed Pericardium Hydrogels To Promote Wound Healing in Vascular Applications. Biomacromolecules 2017, 18 (11), 3802–3811. [PubMed: 28976740]

55. McLoughlin SY; Kastantin M; Schwartz DK; Kaar JL, Single-molecule resolution of protein structure and interfacial dynamics on biomaterial surfaces. PNAS 2013, 110 (48), 19396–19401. [PubMed: 24235137]

56. Langdon BB; Kastantin M; Schwartz DK, Surface Chemistry Influences Interfacial Fibrinogen Self-Association. Biomacromolecules 2015, 16, 3201–3208. [PubMed: 26327275]

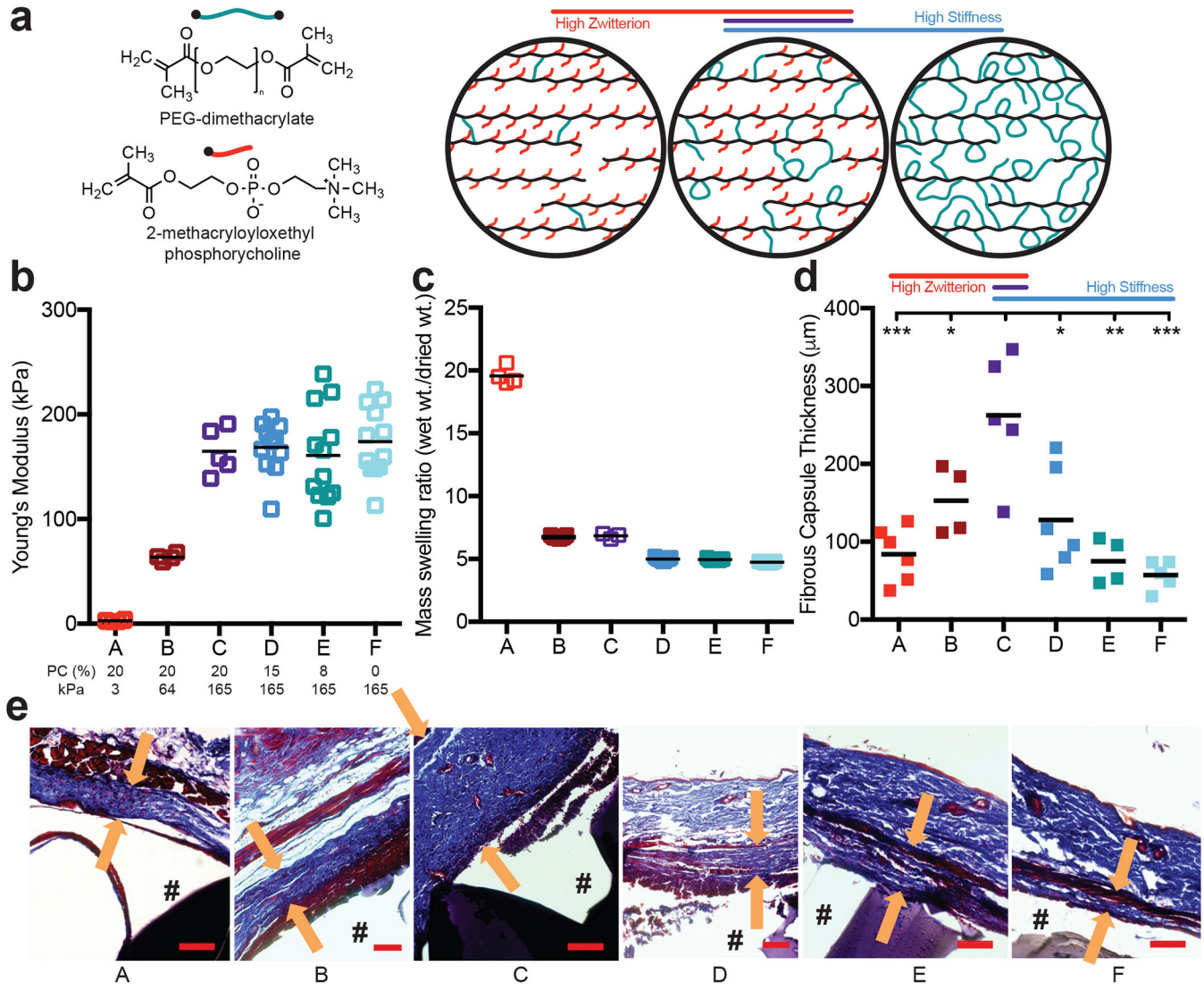

Figure 1. The FBR to PEG hydrogels is highest on stiff, highly zwitterionic implants.

a) A schematic of the hydrogel composed of PEG-dimethacrylate (PEG, green) and 2-methacryloxyloxethyl phosphorycholine (PC, red) to produce a polymer backbone chain (black) with pendant PC groups and PEG crosslinks. b) The Young's modulus and c) mass swelling ratio of the different hydrogel conditions as both PEG and PC content was modulated (N≥4). The molar percentage of PC and the Young's modulus for each hydrogel is labeled below b. d) 28 days after hydrogels were subcutaneously implanted into a mouse, the fibrous capsule thickness was measured using a Masson's Trichrome stain (N≥4). The asterisks indicate significance from hydrogel condition C. e) Representative images for each stain, where "#" denotes the location of the hydrogel, and the arrows represent the thickness measurement taken (scale bar = 100 μm). Significance was determined using an ANOVA with Tukey's post-test, where p=0.05 was considered significant.

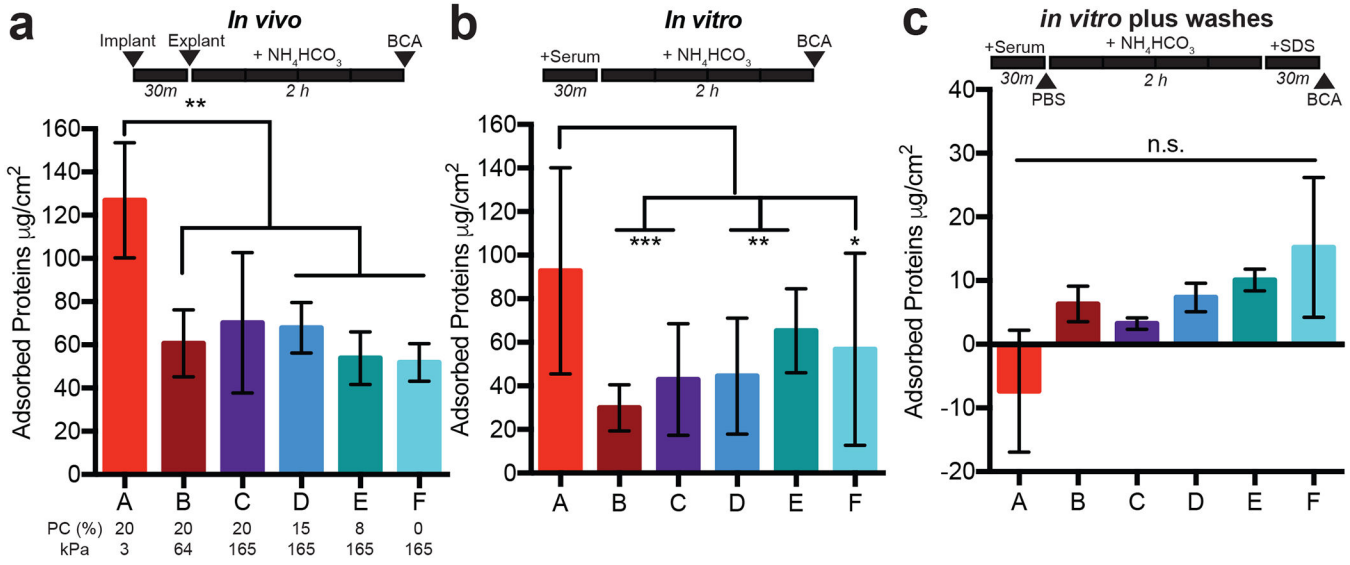

Figure 2. Total protein adsorption to hydrogels is not sufficient to explain the FBR.

A protein assay was used to quantify the amount of protein adsorbed to each hydrogel after a) *in vivo* implantation, b) exposure to 10% serum protein in PBS *in vitro*, or c) with a PBS and 1wt% SDS wash added after exposure to 10% serum proteins *in vitro*. All hydrogels were exposed to ammonium bicarbonate (NH_4HCO_3) for 2 hours before analysis with a bicinchoninic acid assay (BCA). The wash timeline is depicted above each graph.

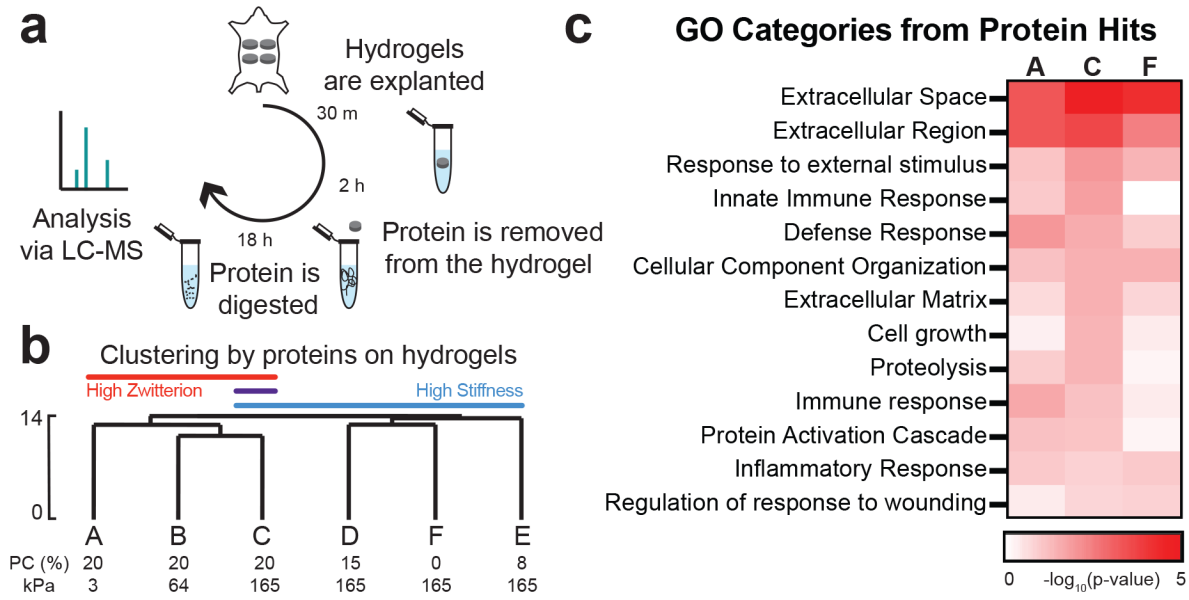

Figure 3. Identity of adsorbed proteins distinguishes highly zwitterionic from stiff hydrogels.

a) Schematic of how protein was collected from implants and analyzed via LC-MS. b) Hierarchical clustering of LC-MS data normalized by the type of protein adsorbed to each hydrogel. The percentage of PC content and the Young's modulus for each hydrogel is labeled below. The scale depicted on the side is the Euclidean distance. c) Heat map of the $\log_{10}$(p-value) for select Gene Ontology (GO) categories identified from the proteins that adhered to hydrogels A, C, and F. These were identified using DAVID with all proteins identified as the background.

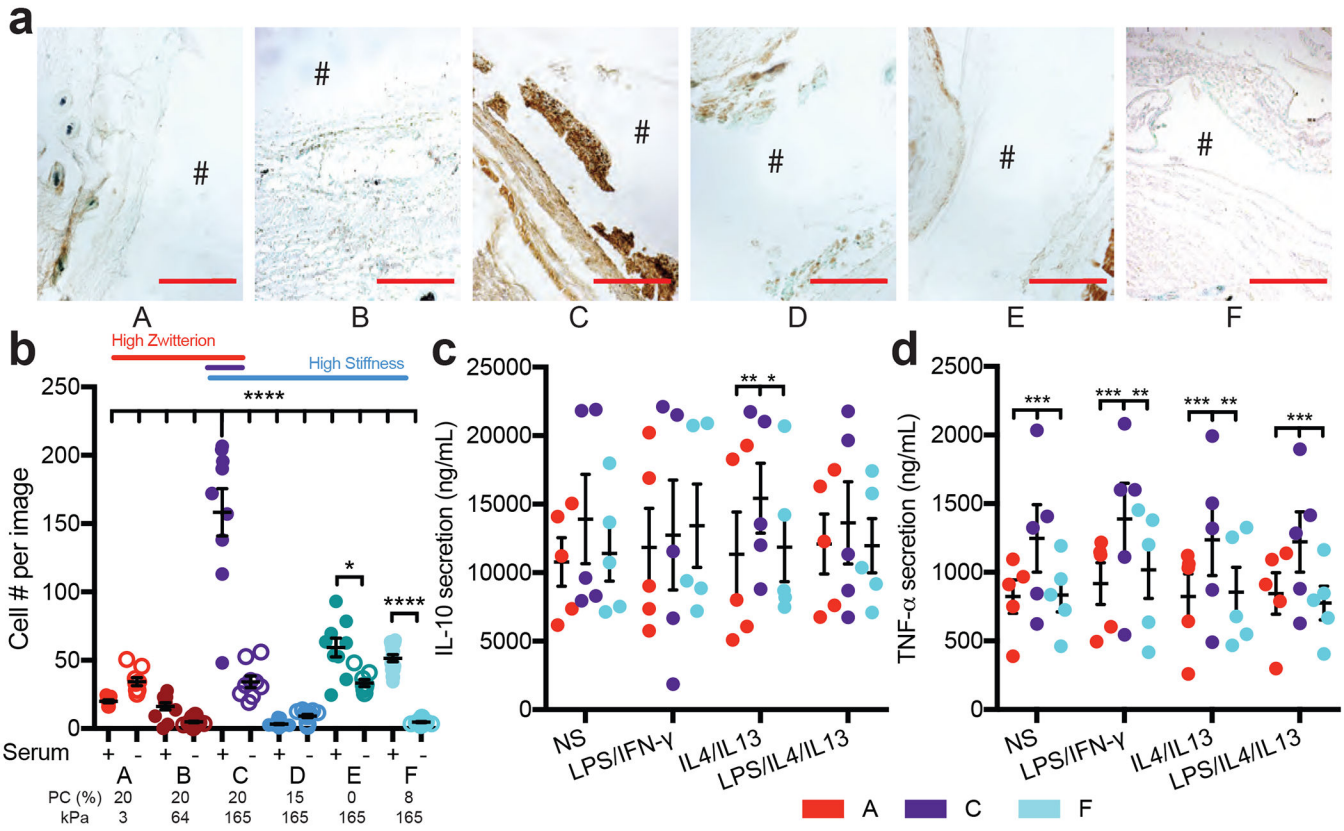

Figure 4. Macrophages adhere better to implants with a more severe foreign body response.

a) Representative images for macrophages stained around the implant, where the # denotes the location of the implant (scale 250 μm). b) Cell adhesion to hydrogels either treated for 30 minutes with serum proteins or not and then seeded with macrophages and imaged 24 hours later (N=2, n=4). Stats displayed for plus and minus serum on hydrogels and hydrogel C plus serum compared to all other hydrogels. Secretion of c) IL-10 and d) TNF-alpha from macrophages seeded on hydrogels with different stimulation factors. Stimulation of each condition was as follows: NS: no stimulation, LPS/IFN-γ: 1ng/mL LPS and IFN-γ, IL4/IL13: 20ng/mL IL4 and IL13, LPS/IL4/IL13: 0.5ng/mL LPS and 20ng/mL IL4 and IL13. The percentage of PC content and the Young's modulus for each hydrogel is labeled below. Significance is determined using an ANOVA with Tukey's post-test where p=0.05 is significant. Error bars are the SD (N=2, n=5).

Table 1.

Polymer composition and Young's modulus for hydrogel implants

Gel Name	PC (wt%)	PEG (wt%)	Modulus (kPa) ± SD
A	20	1	3 ± 1
B	20	4	64 ± 4
C	20	6	165 ± 22
D	15	8	169 ± 25
E	8	12	161 ± 45
	0	18.4	174 ± 34